

# Selective observation of spin and charge dynamics in an organic superconductor $\lambda$ -(BETS)<sub>2</sub>GaCl<sub>4</sub> using <sup>69,71</sup>Ga NMR measurements

T. Kobayashi<sup>1,\*</sup>, K. Tsuji,<sup>2</sup> A. Ohnuma,<sup>2</sup> and A. Kawamoto<sup>1,2</sup>

<sup>1</sup>Graduate School of Science and Engineering, Saitama University, Saitama 338-8570, Japan

<sup>2</sup>Department of Condensed Matter Physics, Graduate School of Science, Hokkaido University, Sapporo 060-0810, Japan

(Received 1 September 2020; revised 20 November 2020; accepted 23 November 2020; published 15 December 2020)

For the unconventional organic superconductor  $\lambda$ -(BETS)<sub>2</sub>GaCl<sub>4</sub> [BETS = bis(ethylenedithio)tetraselenafulvalene], the importance of both spin and charge degrees of freedom has been discussed based on the broadening of the NMR linewidth due to charge disproportionation and the occurrence of a spin-density-wave phase near the superconducting phase. NMR with the nuclear spin of 1/2, previously used for studying organic conductors, is an effective method for revealing electronic states microscopically; however, it cannot distinguish between charge and spin anomalies. To resolve this problem, in this paper, we performed <sup>69,71</sup>Ga-NMR measurements, which enabled us to study both charge and spin dynamics using different gyromagnetic ratios and quadrupole moments between two isotopes. The spin-lattice relaxation rate is dominated by electric-field gradient fluctuations originating from molecular dynamics above 150 K and, below this temperature, it is dominated by spin fluctuations derived from the  $\pi$  electrons of BETS layers. This change in the relaxation mechanism is considered to be due to the development of interactions between GaCl<sub>4</sub> ions and BETS layers upon freezing of the molecular motion by cooling. Below 150 K, the contribution of spin fluctuations monotonically increases, and no increase in the charge fluctuation was observed, suggesting that the spin degree of freedom plays a major role in low-temperature physical properties. Our findings will aid theoretical studies on superconducting properties.

DOI: [10.1103/PhysRevB.102.235131](https://doi.org/10.1103/PhysRevB.102.235131)

## I. INTRODUCTION

In organic conductors, the competition between a relatively narrow bandwidth and Coulomb repulsion causes various physical phenomena in which charge–spin entanglement occurs. Most representative organic conductors, such as  $\kappa$ -(ET)<sub>2</sub>X [ET and X denote bis(ethylenedithio)tetrathiafulvalene and monovalent anion, respectively], have a dimeric structure of ET molecules and are regarded as systems with an effective half-filled band. Depending on the ratio between the bandwidth and on-site Coulomb repulsion, a system transforms from a Mott insulator/antiferromagnet to a metal/superconductor [1]. Accordingly, electronic spin plays a major role in the dimer-Mott system; however, physical properties originating from the charge degree of freedom have also been recently observed. For example, dielectric anomalies in many types of  $\kappa$ -type organic insulators [2–4], charge ordering and a quantum dipole liquid in  $\kappa$ -(ET)<sub>2</sub>Hg(SCN)<sub>2</sub>Y (Y = Cl, Br) [5–8], and a mysterious physical property called the 6 K anomaly in the quantum-spin-liquid candidate  $\kappa$ -(ET)<sub>2</sub>Cu<sub>2</sub>(CN)<sub>3</sub> [9,10], have been reported. These phenomena have attracted considerable attention from the perspective of multiferroicity.

Quasi-two-dimensional organic charge transfer salts, such as  $\lambda$ -(BETS)<sub>2</sub>MCl<sub>4</sub> [M = Ga, Fe; BETS: bis(ethylenedithio)tetraselenafulvalene], are also dimerized

systems; further, they exhibit exotic properties such as the Fulde–Ferrell–Larkin–Ovchinnikov superconducting (SC) state [11–14], magnetic-field-induced superconductivity [15,16], and  $\pi$ - $d$  interaction-induced metal–insulator transition with antiferromagnetic ordering [17]. In these systems, the contributions of both spin and charge degrees of freedom to the physical properties have been reported.  $\lambda$ -(BETS)<sub>2</sub>FeCl<sub>4</sub> exhibits dielectric anomalies below 70 K [18], provoking discussions regarding charge disproportionation. These anomalies were also detected by x-ray diffraction and <sup>1</sup>H-nuclear magnetic resonance (NMR) measurements [19,20]. Moreover, <sup>77</sup>Se-NMR measurements for  $\lambda$ -(BETS)<sub>2</sub>GaCl<sub>4</sub> and  $\lambda$ -(BETS)<sub>2</sub>FeCl<sub>4</sub> have revealed line broadening at low temperatures, indicating charge disproportionation [21,22].

Regarding the physical properties derived from the spin degree of freedom,  $\lambda$ -(BETS)<sub>2</sub>GaBr<sub>x</sub>Cl<sub>4–x</sub> with  $x = 0.75$  exhibits divergence of the spin-lattice relaxation rate divided by temperature  $(T_1 T)^{-1}$  with a metal–insulator transition at 13 K, indicating spin-density wave (SDW) ordering [23]. The salt with  $x = 0.75$  is located much closer to the SC salt  $\lambda$ -(BETS)<sub>2</sub>GaCl<sub>4</sub> ( $x = 0$ ) in the phase diagram of  $\lambda$ -(BETS)<sub>2</sub>GaBr<sub>x</sub>Cl<sub>4–x</sub> [24,25]; in the latter,  $(T_1 T)^{-1}$  increases with a decrease in temperature below 10 K when the superconductivity is suppressed by the magnetic field [21,26,27]. Therefore, an increase in  $(T_1 T)^{-1}$  of the SC salt is considered to represent the spin fluctuation derived from the adjacent SDW phase. The experimental results discussed above indicate the importance of both spin and charge degrees of

\*tkobayashi@phy.saitama-u.ac.jp

freedom; however, the dominant one between these two cannot be determined. We believe that distinctly investigating the spin and charge contributions is important for understanding the physical properties of charge–spin entanglement in organic conductors, including clarification of the SC mechanism of  $\lambda$ -type salts.

Although  $^{13}\text{C}$  and  $^{77}\text{Se}$  NMR are powerful methods for revealing electronic states microscopically, they cannot distinguish between charge and spin anomalies because they are magnetic probes having a nuclear spin of  $I = 1/2$ , and charge anomalies are observed via a local magnetic field. Therefore, to separately investigate the spin and charge properties of  $\lambda$ -(BETS) $_2\text{GaCl}_4$ , in this paper, we focus on NMR spectroscopy utilizing the Ga nuclei in the insulating layer. Two isotopes of Ga, namely,  $^{69}\text{Ga}$  and  $^{71}\text{Ga}$ , exist, whose nuclear spin  $I$  is  $3/2$ . They have different gyromagnetic ratios  $^n\gamma$  and quadrupole moments  $^nQ$  ( $n = 69, 71$ ) and their relationship is as follows:  $^{71}\gamma > ^{69}\gamma$  and  $^{71}Q < ^{69}Q$ . Therefore,  $^{71}\text{Ga}$  and  $^{69}\text{Ga}$  NMR are more sensitive to magnetic and charge anomalies, respectively. Actually, NMR measurements using different isotopes is a well-established technique [28–31], and the charge and magnetic anomalies can be distinguished by comparing the  $^{69,71}\text{Ga}$ -NMR results. In this paper, we conduct a  $^{69,71}\text{Ga}$ -NMR study on  $\lambda$ -(BETS) $_2\text{GaCl}_4$  and demonstrate that NMR measurements using nuclei with  $I > 1/2$  will be effective for investigating the physical phenomena of organic conductors, where charge and spin degrees of freedom are highly entangled with each other.

## II. EXPERIMENTS

Single crystals of  $\lambda$ -(BETS) $_2\text{GaCl}_4$  salt were prepared electrochemically [32]. NMR measurements were performed on  $^{69}\text{Ga}$  ( $^{69}\gamma/2\pi = 10.219$  MHz/T,  $^{69}Q = 0.171$  barns) and  $^{71}\text{Ga}$  ( $^{71}\gamma/2\pi = 12.984$  MHz/T,  $^{71}Q = 0.107$  barns) nuclei under a magnetic field of 6.4 T for powder samples made from moderately crushed single crystals. The  $^{69,71}\text{Ga}$ -NMR spectra were obtained via the fast Fourier transformation (FFT) of the echo signals following a  $\pi/2 - \pi$  pulse sequence with a typical  $\pi/2$  pulse length of 3  $\mu\text{s}$ . The spin-lattice relaxation time  $T_1$  was measured using the conventional saturation recovery method for the central transition  $1/2 \leftrightarrow -1/2$ .  $T_1$  was determined by fitting the magnetization recovery curves using the function  $1 - M(t)/M(\infty) = 0.1 \exp(-t/T_1) + 0.9 \exp(-6t/T_1)$ , where  $M(t)$  and  $M(\infty)$  denote the nuclear magnetization at time  $t$  after the saturation and the nuclear magnetization at equilibrium ( $t \rightarrow \infty$ ), respectively.

## III. RESULTS

The crystal structure of  $\lambda$ -(BETS) $_2\text{GaCl}_4$  is composed of alternating layers of conducting BETS molecules and insulating  $\text{GaCl}_4^-$  anions, as shown in Fig. 1. In a unit cell, there are two Ga sites which are connected by an inversion center, so one magnetically inequivalent site is expected. Since Ga ions exist in tetrahedral environments, electric field gradient (EFG) at the Ga sites is expected to be zero.

Figure 2 shows the  $^{69}\text{Ga}$ -NMR spectrum at 80 K, obtained by the summation of the FFT spectrum as a function of fre-

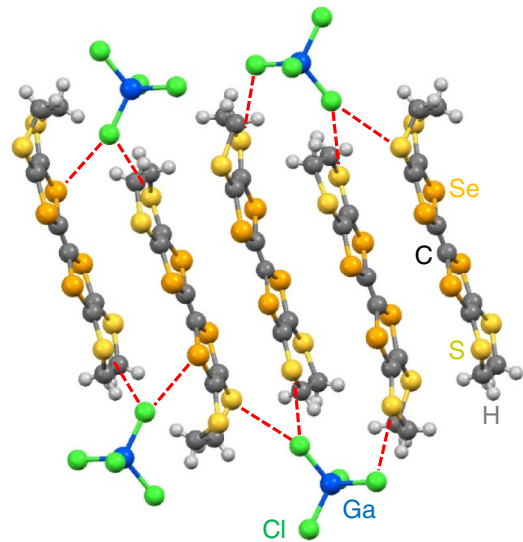


FIG. 1. Crystal structure of  $\lambda$ -(BETS) $_2\text{GaCl}_4$  [25]. Dashed lines denote the Se/S $\cdots$ Cl contacts shorter than the sum of the van der Waals radii.

quency. Sharp central peaks (inset of Fig. 2) and two broad satellite peaks at approximately 61.4 and 62.9 MHz were observed in the spectrum. This spectrum can be described by the nuclear spin Hamiltonian as follows:

$$\begin{aligned} \mathcal{H} &= \mathcal{H}_Z + \mathcal{H}_Q \\ &= -^n\gamma \hbar \mathbf{H} \cdot \mathbf{I} + \frac{\hbar \omega_Q}{6} \left[ 3I_z^2 - I^2 + \frac{\eta}{2} (I_+^2 + I_-^2) \right], \quad (1) \end{aligned}$$

where  $\mathcal{H}_Z$  and  $\mathcal{H}_Q$  represent the nuclear Zeeman interaction and electric quadrupole interaction, respectively;  $\mathbf{H}$  denotes the external magnetic field,  $\hbar$  is the reduced Planck's constant,  $\eta$  is the asymmetry parameter of the EFG, and  $\omega_Q$  denotes

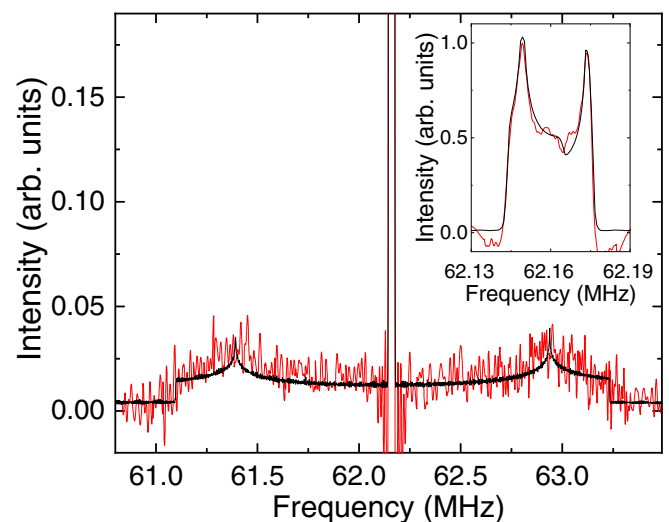


FIG. 2. (a)  $^{69}\text{Ga}$ -NMR powder spectrum measured at 80 K. Inset shows the entire central spectrum in a magnified view. The vertical axis is normalized by the maximum of the center peak. Solid line represents the calculated spectra with  $\omega_Q/2\pi = 1.84$  MHz and  $\eta = 0.14$ .

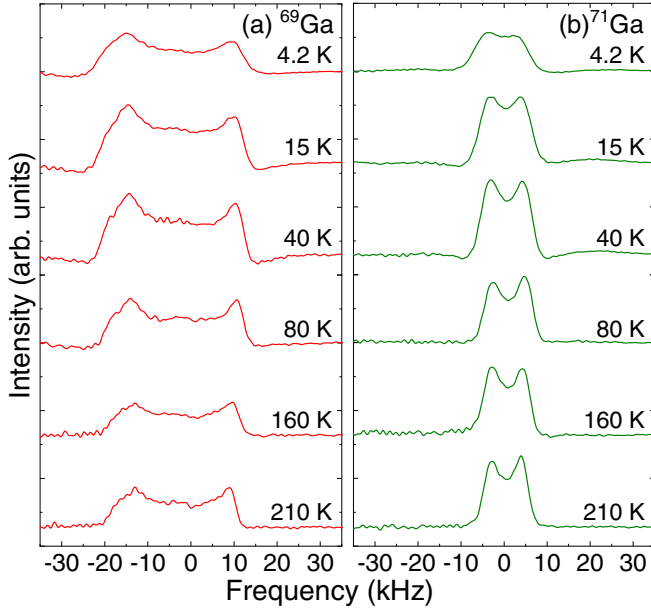


FIG. 3. Central spectra of (a)  $^{69}\text{Ga}$  and (b)  $^{71}\text{Ga}$  NMR at several temperatures.

the nuclear quadrupole frequency.  $\omega_Q$  is defined by  $\omega_Q = e^{\eta} QV_{ZZ}/2\hbar$ , where  $e$  and  $V_{ZZ}$  represent the elementary charge and principal axis of the EFG, respectively. In this measurement,  $\omega_Q$  is small due to symmetry reasons; therefore,  $\mathcal{H}_Z$  is significantly larger than  $\mathcal{H}_Q$ . The solid line represents the simulated powder pattern spectrum with  $\omega_Q/2\pi = 1.84$  MHz and  $\eta = 0.14$  when the term  $\mathcal{H}_Q$  is treated as a perturbation, which reasonably reproduces the observed spectrum. The finite  $\omega_Q$  originates from EFG created by adjacent ions and a slightly distorted tetrahedral coordination of  $\text{GaCl}_4^-$  ions because Ga sites exist in a general position crystallographically [33].

The temperature dependencies of  $^{69,71}\text{Ga}$ -NMR spectra were measured for the central peaks (Fig. 3), where spectral shifts are relative to the  $^{69,71}\text{Ga}$ -resonance frequency of tetrabutylammonium  $\text{GaCl}_4$  dissolved in ethanol. The splitting between two peaks in the  $^{69}\text{Ga}$ -NMR spectra is larger than that in the  $^{71}\text{Ga}$ -NMR spectra because the width is proportional to  $\omega_Q$  [34]. No significant spectral change was observed in the whole temperature range except for the  $^{71}\text{Ga}$ -NMR spectrum at 4.2 K, where the characteristic spectral splitting due to second-order quadrupole perturbation becomes less prominent (discussed in Sec. IV C).

Figure 4 shows the temperature dependencies of  $T_1^{-1}$  of  $^{69,71}\text{Ga}$  NMR,  $^{69}T_1^{-1}$ , and  $^{71}T_1^{-1}$  in the high-temperature region. Above 150 K,  $^{69,71}T_1^{-1}$  strongly depends on the temperature, exhibiting peak behaviors at 300 K and shoulder-like structures at 220 K. The absolute values of  $^{69}T_1^{-1}$  are larger than those of  $^{71}T_1^{-1}$  above 150 K. In contrast, the relation  $^{69}T_1^{-1} > ^{71}T_1^{-1}$  at high temperatures is reversed below approximately 120 K, as shown in Fig. 5, in which  $(^{69,71}T_1 T)^{-1}$  is plotted as a function of temperature. Note that this plot is convenient for discussing the relaxation rate originating from the dynamical susceptibility of electrons as discussed later. Below 120 K, although the absolute values of  $(^{69,71}T_1 T)^{-1}$  are significantly smaller than those at

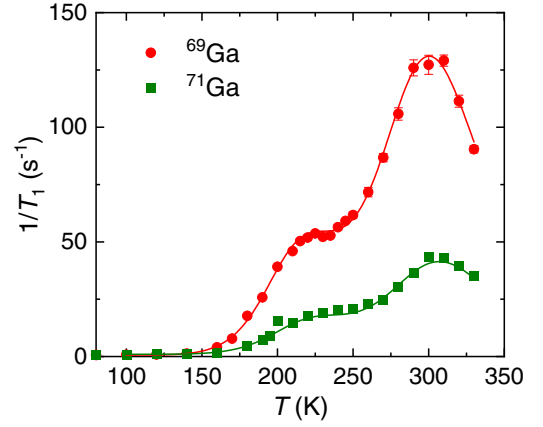


FIG. 4. Temperature dependencies of  $^{69,71}T_1^{-1}$  at high-temperature region. Solid lines denote the fitting curves obtained using Eq. (3).  $^{69}T_1^{-1}$  is larger than  $^{71}T_1^{-1}$  above 150 K, indicating that EFG fluctuations are dominant.

high temperatures, we observed a characteristic temperature dependence of  $(^{69,71}T_1 T)^{-1}$  exhibiting peaks at 50 K and enhancements below 20 K. These behaviors were also observed in  $(T_1 T)^{-1}$  of  $^{13}\text{C}$  NMR, i.e.,  $(^{13}T_1 T)^{-1}$  (inset of Fig. 5) [26].

## IV. DISCUSSION

### A. High-temperature region

The results of  $^{69}T_1^{-1} > ^{71}T_1^{-1}$  at high temperatures indicate that quadrupolar relaxation is the dominant relaxation mechanism, because  $^{69}Q > ^{71}Q$ . In a system without magnetic fluctuations, quadrupole relaxation due to lattice vibration is expected, where  $T_1^{-1}$  shows  $T^2$  dependence at  $T \gg \Theta$  and  $T^7$  dependence at  $T \ll \Theta$  [28]. Here,  $\Theta$  denotes the Debye temperature and it has been estimated as approximately 200 K in  $\lambda$ -(BETS) $_2\text{GaCl}_4$  [35]. This mechanism cannot explain the present results, i.e., the strong dependence of

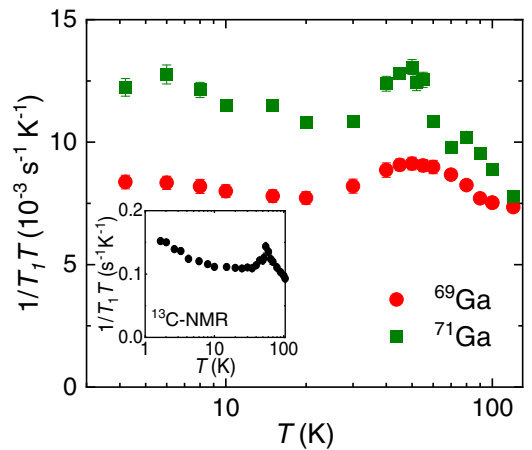


FIG. 5. Temperature dependencies of  $(^{69,71}T_1 T)^{-1}$  at low-temperature region. Contrary to that in a high-temperature region,  $(^{69}T_1 T)^{-1}$  is smaller than  $(^{71}T_1 T)^{-1}$ , indicating that magnetic fluctuations are dominant. Inset shows the temperature dependence of  $(^{13}T_1 T)^{-1}$  [26].

TABLE I. Fitting parameters of Eq. (3) for  ${}^{69}\text{Tl}^{-1}$  in high-temperature region.

	$E_{A,i}/k_B$ (10 <sup>3</sup> K)	$\tau_{0,i}$ (10 <sup>-13</sup> s)	$\langle \omega_{Q,i}^2 \rangle^{1/2}/2\pi$ (kHz)
$i = 1$	1.9(1)	1.8(8)	128(2)
$i = 2$	3.2(2)	0.4(2)	206(2)

${}^{69,71}\text{Tl}^{-1}$  on temperature. Alternatively, it appears that the behavior of  $T_1^{-1}$  possessing a local maximum could be explained by the well-known Bloembergen–Purcell–Pound (BPP) theory [36]. Here, we assumed that thermally activated random fluctuations of  $\text{GaCl}_4^-$  ions at different equilibrium positions modulate the EFG at the Ga sites. In this case,  $T_1^{-1}$  can be approximately given by [28,37,38]

$$\frac{1}{T_1} = \frac{\langle \omega_Q^2 \rangle}{50} \left( \frac{\tau_c}{1 + \omega_L^2 \tau_c^2} + \frac{4\tau_c}{1 + 4\omega_L^2 \tau_c^2} \right), \quad (2)$$

where  $\langle \omega_Q^2 \rangle$  is an effective root-mean-square quadrupole coupling frequency due to the modulation of EFG at different equilibrium positions and  $\omega_L$  is the Larmor frequency. The factor of  $\frac{1}{50}$  corresponds to  $\frac{3}{200} \frac{2I+3}{I^2(2I-1)}$  with  $I = 3/2$ . Generally, the correlation time  $\tau_c$  is described by the Arrhenius-type temperature dependence  $\tau_c = \tau_0 \exp(E_A/k_B T)$  with a prefactor  $\tau_0$ , activation energy of molecular motion  $E_A$ , and Boltzmann constant  $k_B$ . Because  ${}^{69,71}\text{Tl}^{-1}$  exhibited peak behaviors with shoulderlike anomalies, the temperature dependence of  ${}^{69,71}\text{Tl}^{-1}$  above 100 K can be explained by Eq. (3) by including the constant term  ${}^n T_{1,m}^{-1}$  derived from the magnetic fluctuation:

$$\frac{1}{{}^n T_1} = \sum_{i=1,2} \frac{\langle \omega_{Q,i}^2 \rangle}{50} \left( \frac{\tau_{c,i}}{1 + {}^n \omega_L^2 \tau_{c,i}^2} + \frac{4\tau_{c,i}}{1 + 4 {}^n \omega_L^2 \tau_{c,i}^2} \right) + \frac{1}{{}^n T_{1,m}}, \quad (3)$$

where  $\tau_{c,i} = \tau_{0,i} \exp(E_{A,i}/k_B T)$  and  $n = 69, 71$ . As indicated by the solid lines in Fig. 4, the experimental data can be well-reproduced by the parameters listed in Table I, and  ${}^{69}\text{Tl}_{1,m}^{-1} = 0.6(2) \text{ s}^{-1}$  and  ${}^{71}\text{Tl}_{1,m}^{-1} = 0.9(2) \text{ s}^{-1}$ . The parameters with the index  $i = 1$  and 2 are responsible for an anomaly at 220 K and a maximum at 300 K, respectively. Note that  $E_{A,i}$  and  $\tau_{0,i}$  are the common parameters between  ${}^{69}\text{Tl}^{-1}$  and  ${}^{71}\text{Tl}^{-1}$ .  ${}^{69}\omega_L/2\pi$  and  ${}^{71}\omega_L/2\pi$  are fixed at 62.145 MHz and 78.964 MHz, respectively. The ratio between  $\langle \omega_{Q,i}^2 \rangle$  and  $\langle \omega_{Q,i}^2 \rangle$  is fixed because they are proportional to  $nQ^2$ .

Now, we discuss the mechanism of EFG fluctuation that causes the BPP-like behavior. In this regard, three possible mechanisms can be considered: reorientational motion of  $\text{GaCl}_4^-$  ions, vibrational motion within  $\text{GaCl}_4^-$  ions, and translational motion. In the first case, we expected the spectra at high temperatures to be changed by motional narrowing when the correlation time changes exponentially [33]. However, the spectral shape remains unchanged (Fig. 3), suggesting that the contribution of rotation to high-temperature relaxation is small. Vibrational modes of  $\text{GaCl}_4^-$  ions have been investigated by Raman spectroscopy and their frequencies are in the range of 114–386  $\text{cm}^{-1}$  [39], which is significantly higher than

the time scale of NMR frequency. As a result, the effect of the vibrational motion within  $\text{GaCl}_4^-$  ions averages out on the NMR timescale. Therefore, the translational motion is most probably an origin of EFG fluctuation.

Such dynamics can be induced by thermal vibration of the terminal ethylene end groups of BETS molecules, which is known as ethylene motion. Considering that  $\text{GaCl}_4^-$  ions are close to the ethylene end groups in  $\lambda$ -(BETS)<sub>2</sub> $\text{GaCl}_4$ , ethylene motion could induce the translational motion of  $\text{GaCl}_4^-$  ions. In fact, the ethylene motion has been reported in several ET-based organic conductors by many experiments, such as <sup>1</sup>H NMR [40,41]. The parameters of  $E_{A,2}/k_B$  and  $\tau_{0,2}$  are comparable to those of  $\beta'$ -(ET)<sub>2</sub>ICl<sub>2</sub> ( $E_A/k_B \sim 4000$  K and  $\tau_0 \sim 1.2 \times 10^{-14}$  s) [41], suggesting that EFG fluctuation in  $\lambda$ -(BETS)<sub>2</sub> $\text{GaCl}_4$  originates from the dynamics of ethylene groups. Two modes of dynamics represented by  $i = 1, 2$  could originate from two crystallographically inequivalent BETS molecules in  $\lambda$ -(BETS)<sub>2</sub> $\text{GaCl}_4$ . In fact, in  $\kappa$ -(ET)<sub>2</sub>Cu(NCS)<sub>2</sub>, two peaks of the spin–spin relaxation rate derived from the ethylene motion have been observed in <sup>13</sup>C NMR [42].

## B. Low-temperature region

$({}^{71}\text{Tl}T)^{-1}$  is larger than  $({}^{69}\text{Tl}T)^{-1}$  below 120 K (Fig. 5), in contrast to that in the high-temperature region. This result indicates that the magnetic relaxation becomes dominant with the suppression of quadrupole relaxation due to the freezing of ethylene motion. The behaviors observed below 120 K are qualitatively the same as those of  $({}^{13}\text{Tl}T)^{-1}$  (inset of Fig. 5) [26], which is direct evidence that the magnetic fluctuation derived from BETS layers is observed even at the Ga sites.  $({}^{69,71}\text{Tl}T)^{-1}$  exhibits peak behaviors at 50 K, which coincides with the inflection point of electrical resistivity as a function of temperature. As discussed in the literature [26], this behavior can be understood as the suppression of antiferromagnetic fluctuations due to the development of the coherence of conduction electrons. The enhancement of  $({}^{69,71}\text{Tl}T)^{-1}$  below 20 K is considered to represent the spin fluctuations derived from the adjacent SDW phase [23].

We now discuss the interactions between  $\pi$  electrons of BETS layers and Ga nuclear spins responsible for the observed magnetic fluctuations.  $(T_1 T)^{-1}$  owing to the spin fluctuation of electrons can be generally written as [43]

$$\frac{1}{T_1 T} = \frac{2^n \gamma^2 k_B}{\gamma_e^2 \hbar^2} \sum_{\mathbf{q}} |A_{\mathbf{q}}|^2 \frac{\chi''(\mathbf{q})}{\omega_L}, \quad (4)$$

where  $\gamma_e$ ,  $A_{\mathbf{q}}$ , and  $\chi''(\mathbf{q})$  denote the electron gyromagnetic ratio, wave vector  $\mathbf{q}$ -dependent hyperfine coupling constant, and imaginary part of dynamical susceptibility, respectively. One possibility for the presence of the hyperfine mechanism is due to the dipole field arising from  $\pi$  electrons. In this case,  $A_{\mathbf{q}}$  can be roughly estimated, and the estimated value of  $T_1^{-1}$  is 100 times smaller than the experimental values, assuming  $0.5\mu_B$  ( $\mu_B$ : Bohr magneton) per BETS molecule and the dynamic susceptibility estimated from the <sup>13</sup>C-NMR results [26]. An alternative mechanism is the exchange interaction between Ga nuclear spins and  $\pi$  spins through Cl ions because a static transferred coupling can form when the ethylene motion is frozen at low temperatures. Furthermore, as discussed in

$\lambda$ -(BETS)<sub>2</sub>FeCl<sub>4</sub> [44,45], many short contacts exist between Se/S $\cdots$ Cl (Fig. 1); in the figure, the contacts shorter than the van der Waals distances of 3.65 Å (Cl $\cdots$ S) and 3.80 Å (Cl $\cdots$ Se) are depicted by dashed lines. The presence of interaction between the conduction electrons and anion molecules suggests a strong  $\pi - d$  interaction in  $\lambda$ -(BETS)<sub>2</sub>FeCl<sub>4</sub> [44]. The above discussion reveals that the magnetic fluctuations of  $\pi$  spins can be detected even at the Ga sites when the quadrupole relaxation is suppressed and a hyperfine coupling between the Ga nuclear spins and  $\pi$  spins is established.

### C. Fluctuation at temperatures immediately above $T_c$

To elucidate the mechanism of superconductivity, understanding the electronic state for temperatures immediately above the SC transition temperature  $T_c$  is important. Here, we compare our results with the previous NMR results for  $\lambda$ -(BETS)<sub>2</sub>GaCl<sub>4</sub> in the low-temperature region. In <sup>77</sup>Se NMR measurements, an anomalous line broadening has been observed [21]. Because the angular dependence of the linewidth is proportional to that of the Knight shift, it has been suggested that the charge disproportionation contributes to line broadening, where the charge density is assumed to be proportional to the spin density [21]. Although information on charge distribution cannot be obtained directly by NMR using  $I = 1/2$  nuclei, it can be discussed based on the change in the hyperfine coupling constant. It has been indicated that <sup>13</sup>C NMR quantitatively agrees with <sup>77</sup>Se NMR [26]. In addition, the temperature dependence of the <sup>13</sup>C-NMR spectra indicates that anomalous line broadening occurs below 20 K and  $(^{13}T_1 T)^{-1}$  also exhibits the enhancement below the same temperature, suggesting fluctuation at temperatures immediately above  $T_c$  [26]. <sup>69,71</sup>Ga-NMR measurements also detected the anomalies in the NMR spectra. As shown in Fig. 3, the shape of the <sup>69</sup>Ga-NMR line does not clearly change with temperature, whereas the characteristic line shape of the <sup>71</sup>Ga-NMR spectrum is obscured at 4.2 K, which seems to have been occurring from 15 K. Because the shape of the <sup>71</sup>Ga-NMR line changes below the temperature where the <sup>13</sup>C-NMR linewidth increases, we suggest that the low-temperature line broadening in <sup>71</sup>Ga NMR detects the same phenomenon as that in <sup>13</sup>C and <sup>77</sup>Se NMR. Particularly, the line broadening was clearly observed only in the <sup>71</sup>Ga-NMR spectra. Because <sup>71</sup>Ga NMR is more sensitive to magnetic properties than <sup>69</sup>Ga NMR and vice versa, this broadening is considered to be caused by the spin degree of freedom rather than the charge degree of freedom.

For a comprehensive discussion on whether the spin or charge degrees of freedom are dominant, the isotopic ratio of  $T_1^{-1}$  provides definitive information. Figure 6 shows the temperature dependence of the isotopic ratio of  $T_1^{-1}$ , i.e.,  $^{71}T_1^{-1} / ^{69}T_1^{-1}$ . At high temperatures, the isotopic ratio of  $T_1^{-1}$  is almost temperature independent and consistent with  $(^{71}Q / ^{69}Q)^2 = 0.392$ . However, with a decrease in temperature below approximately 150 K, the isotopic ratio of  $T_1^{-1}$  deviates from  $(^{71}Q / ^{69}Q)^2$ . This result clearly demonstrates that the relaxation mechanism changes from quadrupolar to magnetic because of the freezing of ethylene motion. These results corroborate the discussion in Secs. IV A and IV B.

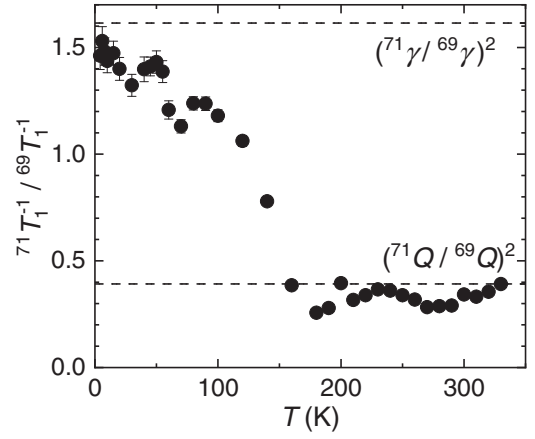


FIG. 6. Temperature dependence of isotopic ratio of the relaxation rates. Dashed lines represent the values of  $(^{71}\gamma / ^{69}\gamma)^2$  and  $(^{71}Q / ^{69}Q)^2$ .

At low temperatures, the isotopic ratio of  $T_1^{-1}$  monotonically increases and approaches  $(^{71}\gamma / ^{69}\gamma)^2 = 1.614$  toward the lowest temperature. These results indicate that magnetic fluctuation is dominant at low temperatures. Through <sup>77</sup>Se- and <sup>13</sup>C-NMR measurements, the anomalous NMR results immediately above  $T_c$  because of electrical and magnetic origins have been discussed [21,26]; however, these experiments cannot distinguish them in principle. The results of  $^{71}T_1^{-1} / ^{69}T_1^{-1}$  suggest that the magnetic fluctuation, and not charge fluctuation, is responsible for the low-temperature physical properties.

Recently, the divergence of  $(^{13}T_1 T)^{-1}$  with a metal-insulator transition was observed in  $\lambda$ -(BETS)<sub>2</sub>GaBr<sub>0.75</sub>Cl<sub>3.25</sub>, indicating that the SDW phase is in the vicinity of the SC phase [23]. Considering the neighboring SDW phase and the present finding of magnetic fluctuations at temperatures immediately above  $T_c$ , a possibility of SDW fluctuation-mediated superconductivity is suggested.

Finally, we comment on the usefulness of NMR experiments using  $I > 1/2$  nuclide. NMR measurements using  $I = 1/2$  nuclide are certainly powerful probes, because the electronic state can be sensitively examined through nuclear spins. However, the information on the charge properties can be obtained only from the change in the hyperfine coupling constants [46]. As discussed in the Appendix, observing the charge fluctuations using spin-1/2 NMR is difficult. Overcoming this problem, NMR measurements using  $I > 1/2$  nuclide that has a finite nuclear quadrupole moment provide significant information about charge dynamics. In fact, we succeeded in detecting the charge anomaly in  $\kappa$ -(ET)<sub>2</sub>Cu<sub>2</sub>(CN)<sub>3</sub> by <sup>63,65</sup>Cu-NQR experiments [10]. This technique will greatly contribute to elucidating the physical properties of systems in which the charge degree of freedom is important, e.g.,  $\beta''$ -(ET)<sub>4</sub>[(H<sub>3</sub>O)Ga(C<sub>2</sub>O<sub>4</sub>)<sub>3</sub>] · C<sub>6</sub>H<sub>5</sub>NO<sub>2</sub> [47,48] and  $\kappa$ -(ET)<sub>2</sub>Hg(SCN)<sub>2</sub>Y (Y = Cl, Br) [5–8], where <sup>69,71</sup>Ga, <sup>35,37</sup>Cl, and <sup>79,81</sup>Br NMR experiments will be appropriate probes.

## V. SUMMARY

We performed  $^{69,71}\text{Ga}$ -NMR measurements on  $\lambda$ -(BETS) $_2\text{GaCl}_4$  to separately investigate the spin and charge dynamics. Quadrupole relaxations originating from molecular dynamics were observed at high temperatures. The temperature dependence of  $^{69,71}T_1^{-1}$  is qualitatively the same as that of  $^{13}T_1^{-1}$  at low temperatures, suggesting that the magnetic fluctuation derived from BETS layers was observed even in the insulating layers. The isotopic ratio of  $T_1^{-1}$  clearly demonstrates the transformation of the relaxation mechanism from quadrupole to magnetic at approximately 150 K. This can be understood by the development of interaction between  $\text{GaCl}_4^-$  ions and BETS molecules upon the freezing of molecular motion by cooling, which will help understand the mechanism of  $\pi$ - $d$  interaction in  $\lambda$ -(BETS) $_2\text{FeCl}_4$ . Using the isotopic ratio of  $T_1^{-1}$ , we found that the magnetic fluctuations gradually become dominant with the decrease in temperature below 120 K, and no significant decrease in the isotopic ratio of  $T_1^{-1}$  was observed. Therefore, the spin degree of freedom plays an important role in low-temperature electronic properties, establishing that the fluctuation immediately above  $T_c$  observed in the previous  $^{13}\text{C}$  NMR is not quadrupolar but magnetic. We suggest that this magnetic fluctuation originates from the SDW fluctuation and plays an important role as a pairing mechanism in superconductivity. This study demonstrated that NMR measurements using  $I > 1/2$  nuclide can distinguish the spin and charge dynamics sensitively, and that they can be applied to investigate many types of organic charge transfer salts that exhibit charge-spin entanglement properties.

## ACKNOWLEDGMENTS

The authors would like to thank S. Fukuoka for his valuable discussion. This work was partially supported by the Japan Society for the Promotion of Science KAKENHI Grants No. 16K05427, No. 18H05843, No. 19K21033, and No. 19K03758.

## APPENDIX: DETECTION OF CHARGE FLUCTUATIONS BY SPIN-1/2 NMR IN ORGANIC CHARGE TRANSFER SALTS

In general,  $T_1^{-1}$  is expressed using a time correlation function of the fluctuating local magnetic field at the nuclei  $\langle \delta H^-(0)\delta H^+(\tau) \rangle$ , as follows [28]:

$$\frac{1}{T_1} = \frac{n\gamma^2}{2} \int_{-\infty}^{\infty} dt \langle \delta H^-(0)\delta H^+(\tau) \rangle e^{-i\omega t}. \quad (\text{A1})$$

That is,  $T_1^{-1}$  is given by the Fourier transform of  $\langle \delta H^-(0)\delta H^+(\tau) \rangle$ . Subsequently, we discuss the contribution of relaxation rate by extracting this term.

When the magnetic relaxation rate is driven by the fluctuations of electronic spins  $\langle \delta M^-(0)\delta M^+(\tau) \rangle$  through the

hyperfine field, the fluctuating local magnetic field can be given by

$$\langle \delta H^-(0)\delta H^+(\tau) \rangle = \langle A\delta M^-(0)A\delta M^+(\tau) \rangle, \quad (\text{A2})$$

where  $A$  is the hyperfine coupling constant.

In inorganic systems, since an electron locates on an atomic orbital and transfers between atomic sites, spin and charge degrees of freedom are coupled/locked together. On the other hand, in organic conductors of the  $D_2X$  type, where  $D$  is a donor molecule and  $X$  is a monovalent anion, the formal charge of the molecule is  $+0.5e$  and one hole spreads on two molecules in the dimeric systems. Therefore, in addition to the global spin degree of freedom of the dimers, there is an additional internal degree of freedom for charge distribution on two molecules. The change of the charge distribution modifies the hyperfine coupling field from the hole on the dimer and the change in  $A$  can be written as  $A[1 \pm \Delta/2]$ , where  $\Delta$  represents the amplitude of charge disproportionation [49]. In this case, the fluctuation of the local magnetic field with the charge fluctuations is expressed as

$$\begin{aligned} & \langle \delta H^-(0)\delta H^+(\tau) \rangle \\ &= \left\langle A \left[ 1 + \frac{\Delta(0)}{2} \right] \delta M^-(0) A \left[ 1 + \frac{\Delta(\tau)}{2} \right] \delta M^+(\tau) \right\rangle \\ &= A^2 \langle \delta M^-(0)\delta M^+(\tau) \rangle \\ &+ A^2 \left\langle \left[ \frac{\Delta(0) + \Delta(\tau)}{2} \right] \delta M^-(0)\delta M^+(\tau) \right\rangle \\ &+ A^2 \left\langle \frac{\Delta(0)\Delta(\tau)}{4} \delta M^-(0)\delta M^+(\tau) \right\rangle, \end{aligned} \quad (\text{A3})$$

where only the term with positive sign is written for simplicity. When the charge fluctuation is absent ( $\Delta = 0$ ), this equation coincides with Eq. (A2). The second term becomes zero because it contains the average of  $\Delta$ . The first and third terms give the relaxations due to pure spin fluctuations and charge fluctuations detected by NMR with spin 1/2 nuclei.

When a typical charge disproportionation occurs, the charge gap opens [46]. Meanwhile, as charge fluctuations develop, the spin-singlet state becomes stable, following which  $\langle \delta M^-(0)\delta M^+(\tau) \rangle$  decreases. On the other hand, the slow down of the charge fluctuation increases the Fourier transform of  $\langle \Delta(0)\Delta(\tau) \rangle$  at NMR frequency; however, the observed quantity is complicated because it is the product of  $\langle \Delta(0)\Delta(\tau) \rangle$  and  $\langle \delta M^-(0)\delta M^+(\tau) \rangle$ . Moreover, because the amplitude of the third term is considered to be  $\sim \Delta^2/4$  times smaller than that of the first term (pure spin fluctuation), observing the charge fluctuation by NMR using  $I = 1/2$  nuclide is difficult. In the case of spin  $> 1/2$  NMR, because the EFG fluctuations that contribute to quadrupole relaxation are directly driven by the charge fluctuations, the Fourier transform of  $\langle \Delta(0)\Delta(\tau) \rangle$  can be detected.

[1] K. Kanoda, *Hyperfine Interact.* **104**, 235 (1997).

[2] M. Abdel-Jawad, I. Terasaki, T. Sasaki, N. Yoneyama, N.

- Kobayashi, Y. Uesu, and C. Hotta, *Phys. Rev. B* **82**, 125119 (2010).
- [3] P. Lunkenheimer, J. Müller, S. Krohns, F. Schrettle, A. Loidl, B. Hartmann, R. Rommel, M. de Souza, C. Hotta, J. A. Schlueter, and M. Lang, *Nat. Mater.* **11**, 755 (2012).
- [4] M. Pinterić, P. Lazić, A. Pustogow, T. Ivek, M. Kuveždić, O. Milat, B. Gumhalter, M. Basletić, M. Čulo, B. Korin-Hamzić, A. Löhle, R. Hübner, M. Sanz Alonso, T. Hiramatsu, Y. Yoshida, G. Saito, M. Dressel, and S. Tomić, *Phys. Rev. B* **94**, 161105(R) (2016).
- [5] N. Drichko, R. Beyer, E. Rose, M. Dressel, J. A. Schlueter, S. A. Turunova, E. I. Zhilyaeva, and R. N. Lyubovskaya, *Phys. Rev. B* **89**, 075133 (2014).
- [6] T. Ivek, R. Beyer, S. Badalov, M. Čulo, S. Tomić, J. A. Schlueter, E. I. Zhilyaeva, R. N. Lyubovskaya, and M. Dressel, *Phys. Rev. B* **96**, 085116 (2017).
- [7] N. Hassan, S. Cunningham, M. Mourigal, E. I. Zhilyaeva, S. A. Torunova, R. N. Lyubovskaya, J. A. Schlueter, and N. Drichko, *Science* **360**, 1101 (2018).
- [8] A. C. Jacko, E. P. Kenny, and B. J. Powell, *Phys. Rev. B* **101**, 125110 (2020).
- [9] R. S. Manna, M. de Souza, A. Brühl, J. A. Schlueter, and M. Lang, *Phys. Rev. Lett.* **104**, 016403 (2010).
- [10] T. Kobayashi, Q.-P. Ding, H. Taniguchi, K. Satoh, A. Kawamoto, and Y. Furukawa, *Phys. Rev. Res.* **2**, 042023(R) (2020).
- [11] M. A. Tanatar, T. Ishiguro, H. Tanaka, A. Kobayashi, and H. Kobayashi, *J. Supercond.* **12**, 511 (1999).
- [12] S. Uji, T. Terashima, M. Nishimura, Y. Takahide, T. Konoike, K. Enomoto, H. Cui, H. Kobayashi, A. Kobayashi, H. Tanaka, M. Tokumoto, E. S. Choi, T. Tokumoto, D. Graf, and J. S. Brooks, *Phys. Rev. Lett.* **97**, 157001 (2006).
- [13] W. A. Coniglio, L. E. Winter, K. Cho, C. C. Agosta, B. Fravel, and L. K. Montgomery, *Phys. Rev. B* **83**, 224507 (2011).
- [14] S. Uji, K. Kodama, K. Sugii, T. Terashima, T. Yamaguchi, N. Kurita, S. Tsuchiya, T. Konoike, M. Kimata, A. Kobayashi, B. Zhou, and H. Kobayashi, *J. Phys. Soc. Jpn.* **84**, 104709 (2015).
- [15] S. Uji, H. Shinagawa, T. Terashima, T. Yakabe, Y. Terai, M. Tokumoto, A. Kobayashi, H. Tanaka, and H. Kobayashi, *Nature* **410**, 908 (2001).
- [16] L. Balicas, J. S. Brooks, K. Storr, S. Uji, M. Tokumoto, H. Tanaka, H. Kobayashi, A. Kobayashi, V. Barzykin, and L. P. Gor'kov, *Phys. Rev. Lett.* **87**, 067002 (2001).
- [17] A. Kobayashi, T. Udagawa, H. Tomita, T. Naito, and H. Kobayashi, *Chem. Lett.* **22**, 2179 (1993).
- [18] H. Matsui, H. Tsuchiya, E. Negishi, H. Uozaki, Y. Ishizaki, Y. Abe, S. Endo, and N. Toyota, *J. Phys. Soc. Jpn.* **70**, 2501 (2001).
- [19] S. Endo, T. Goto, T. Fukase, H. Matsui, H. Uozaki, H. Tsuchiya, E. Negishi, Y. Ishizaki, Y. Abe, and N. Toyota, *J. Phys. Soc. Jpn.* **71**, 732 (2002).
- [20] S. Komiyama, M. Watanabe, Y. Noda, E. Negishi, and N. Toyota, *J. Phys. Soc. Jpn.* **73**, 2385 (2004).
- [21] K. Hiraki, M. Kitahara, T. Takahashi, H. Mayaffre, M. Horvatić, C. Berthier, S. Uji, H. Tanaka, B. Zhou, A. Kobayashi, and H. Kobayashi, *J. Phys. Soc. Jpn.* **79**, 074711 (2010).
- [22] K. Hiraki, H. Mayaffre, M. Horvatić, C. Berthier, S. Uji, T. Yamaguchi, H. Tanaka, A. Kobayashi, H. Kobayashi, and T. Takahashi, *J. Phys. Soc. Jpn.* **76**, 124708 (2007).
- [23] T. Kobayashi, T. Ishikawa, A. Ohnuma, M. Sawada, N. Matsunaga, H. Uehara, and A. Kawamoto, *Phys. Rev. Res.* **2**, 023075 (2020).
- [24] H. Kobayashi, H. Akutsu, E. Arai, H. Tanaka, and A. Kobayashi, *Phys. Rev. B* **56**, R8526 (1997).
- [25] H. Tanaka, A. Kobayashi, A. Sato, H. Akutsu, and H. Kobayashi, *J. Am. Chem. Soc.* **121**, 760 (1999).
- [26] T. Kobayashi and A. Kawamoto, *Phys. Rev. B* **96**, 125115 (2017).
- [27] T. Kobayashi, H. Taniguchi, A. Ohnuma, and A. Kawamoto, *Phys. Rev. B* **102**, 121106(R) (2020).
- [28] A. A. Abragam, *The Principles of Nuclear Magnetism* (Oxford University Press, Oxford, 1961).
- [29] D. F. Holcomb and R. E. Norberg, *Phys. Rev.* **98**, 1074 (1955).
- [30] R. E. Walstedt, W. W. Warren, R. F. Bell, G. F. Brennert, G. P. Espinosa, J. P. Remeika, R. J. Cava, and E. A. Rietman, *Phys. Rev. B* **36**, 5727 (1987).
- [31] T. Imai, T. Shimizu, T. Tsuda, H. Yasuoka, T. Takabatake, Y. Nakazawa, and M. Ishikawa, *J. Phys. Soc. Jpn.* **57**, 1771 (1988).
- [32] H. Kobayashi, T. Udagawa, H. Tomita, K. Bun, T. Naito, and A. Kobayashi, *Chem. Lett.* **22**, 1559 (1993).
- [33] R. W. Schurko, S. Wi, and L. Frydman, *J. Phys. Chem. A* **106**, 51 (2002).
- [34] M. Cohen and F. Reif, *Solid State Phys.* **5**, 321 (1957).
- [35] Y. Ishizaki, H. Uozaki, H. Tsuchiya, Y. Abe, E. Negishi, H. Matsui, S. Endo, and N. Toyota, *Synth. Met.* **133**, 219 (2003).
- [36] N. Bloembergen, E. M. Purcell, and R. V. Pound, *Phys. Rev.* **73**, 679 (1948).
- [37] H. W. Spiess, in *Dynamic NMR Spectroscopy*, Vol. 12 (Springer, Berlin, Heidelberg, 1978), pp. 55–214.
- [38] A. Avogadro, F. Tabak, M. Corti, and F. Borsa, *Phys. Rev. B* **41**, 6137 (1990).
- [39] L. A. Woodward and A. A. Nord, *J. Chem. Soc.* 3721 (1956).
- [40] K. Miyagawa, A. Kawamoto, Y. Nakazawa, and K. Kanoda, *Phys. Rev. Lett.* **75**, 1174 (1995).
- [41] M. Sawada, S. Fukuoka, and A. Kawamoto, *Phys. Rev. B* **97**, 045136 (2018).
- [42] Y. Kuwata, M. Itaya, and A. Kawamoto, *Phys. Rev. B* **83**, 144505 (2011).
- [43] T. Moriya, *J. Phys. Soc. Jpn.* **18**, 516 (1963).
- [44] T. Mori and M. Katsuhara, *J. Phys. Soc. Jpn.* **71**, 826 (2002).
- [45] T. Lee, Y. Oshima, H. Cui, and R. Kato, *J. Phys. Soc. Jpn.* **87**, 114702 (2018).
- [46] K. Miyagawa, A. Kawamoto, and K. Kanoda, *Phys. Rev. B* **62**, R7679 (2000).
- [47] Y. Ihara, M. Jeong, H. Mayaffre, C. Berthier, M. Horvatić, H. Seki, and A. Kawamoto, *Phys. Rev. B* **90**, 121106(R) (2014).
- [48] Y. Ihara, K. Moribe, S. Fukuoka, and A. Kawamoto, *Phys. Rev. B* **100**, 060505(R) (2019).
- [49] S. Hirose and A. Kawamoto, *Phys. Rev. B* **80**, 165103 (2009).